Supporting Online Material for:

A cullin 4B-RING E3 ligase complex fine-tunes pancreatic δ cell paracrine interactions

Qing Li[#1], Min Cui[#1], Fan Yang[#1], Na Li[1], , Baichun Jiang[4], Zhen Yu[1], Daolai Zhang[3], Yijing Wang[3], Xibin Zhu[1], Huili Hu[4], Pei-Shan Li[4], Shang-Lei Ning[3], Si Wang[1], Haibo Qi[1], Hechen Song[1], Dongfang He[1,3], Amy Lin[2], Jingjing Zhang[5], Feng Liu[5], Jiajun Zhao[6], Ling Gao [6], Fan Yi[7], Tian Xue[8], Jin-Peng Sun[2,3], Yaoqin Gong*[4], Xiao Yu*[1]

Corresponding author: Yaoqin Gong (corresponding author)

E-mail: yxg8@sdu.edu.cn

Xiao Yu (corresponding author)

E-mail: yuxiao@sdu.edu.cn

This PDF file includes:

Supplemental Figures： Supplemental Figure 1 to Supplemental Figure 12

Supplemental Tables： Supplemental Table1 to Supplemental Table 2

Supplemental Materials and Methods

Reference

Supplemental Figures

Supplemental Figure 1

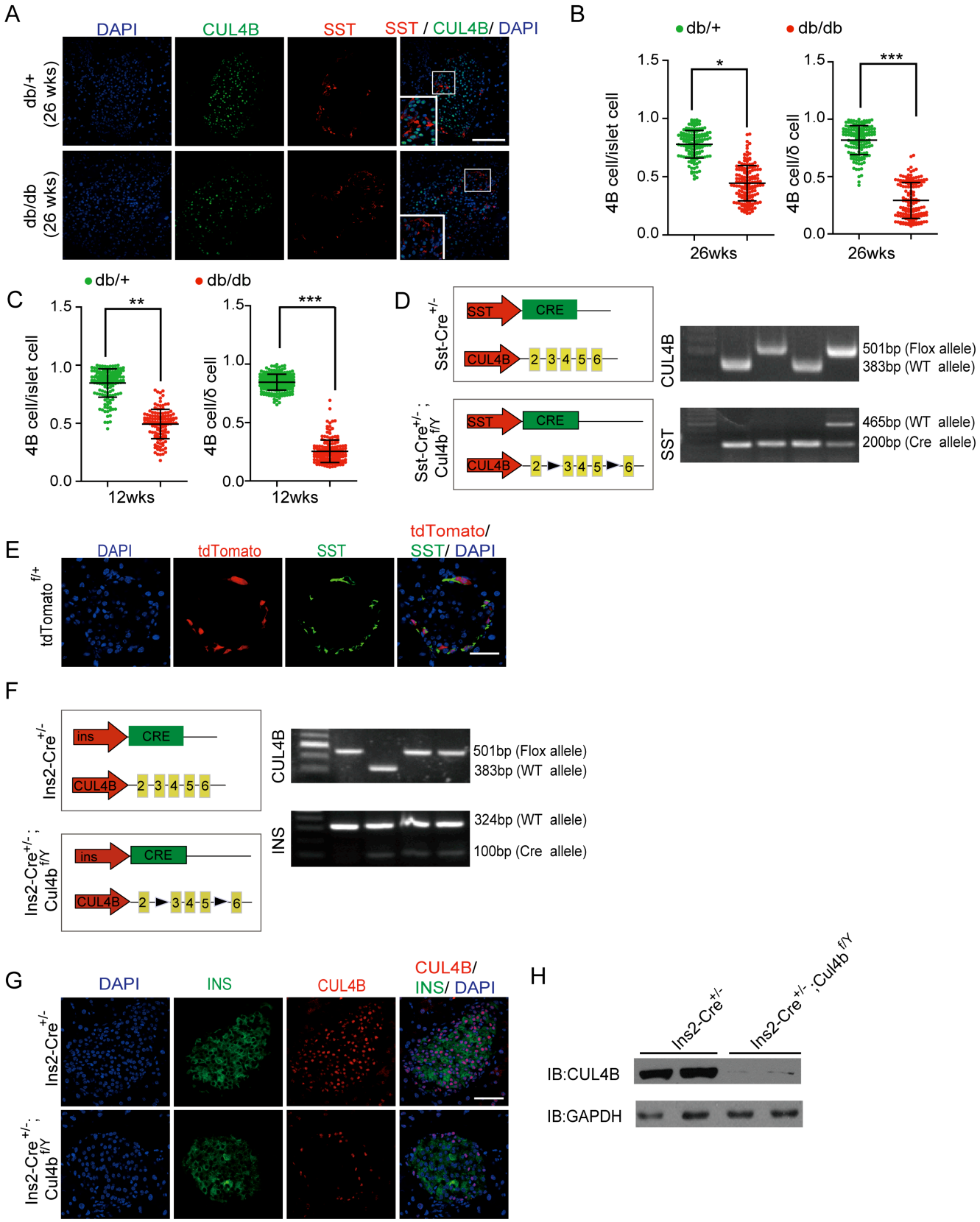

Supplemental Figure 1. (**A**) Immunostaining for CUL4B (green) and somatostatin (red) in pancreatic sections of *db/db* and *db/+* mice (26 weeks). Scale bar, 100 μm. (**B-C**) Statistical data of the ratio of CUL4B expression in total cells or pancreatic δ cells (quantification of the CUL4B immunostaining levels vs. DAPI or somatostatin staining levels from **A** and figure 1**C**) n=6 mice per group; 4-7 random areas were selected from each pancreatic section, and 10 sections were randomly selected from each mouse. (**D**) Left panel: schematic representation of somatostatin-producing cell type-specific cul4b knockout male mice (*SST-cre; Cul4b*^{flox} mice); The LoxP sequences were recognized by the Cre enzyme, the expression of which was driven by the somatostatin promoter (*SST-cre*), thus cleaving exons 3-5 of the Cul4b gene in *SST-cre; Cul4b*^{flox} mice and generating a cul4b knockout in somatostatin-expressing cells. Right panel: PCR analysis of genomic DNA from tails (right panel). (**E**) Immunofluorescence for SST (green) and tdTomato (red) in pancreatic sections of *SST-cre; tdt*^{flox} mice. The results indicated that pancreatic δ cells were specifically labeled in red in *SST-cre; tdt*^{flox} mice. Scale bar, 50μm. (**F**) Left panel: schematic representation of insulin-producing cell type-specific cul4b knockout male mice (*Ins2-cre; Cul4b*^{flox} mice): The LoxP sequences of the *Cul4b-flox* mice were recognized by the Cre enzyme, the expression of which was driven by the insulin promoter (*Ins2-cre*), thereby generating a cul4b knockout specifically in insulin-expressing cells. Right panel: PCR analysis of tail snip genomic DNA. (**G-H**) Confirmation of pancreatic β-cell-specific Cul4b deficiency through immunofluorescence (**G**) and western blotting (**H**). Scale bar, 50μm. A representative western blot from at least 3 independent experiments is shown (**H**). *, $p<0.05$; **, $p<0.01$; *** $p<0.001$; *db/db* mice were compared with their *db/+* littermates. The bars represent mean±s.d. All data statistics were analysed using one-way ANOVA.

Supplemental Figure 2

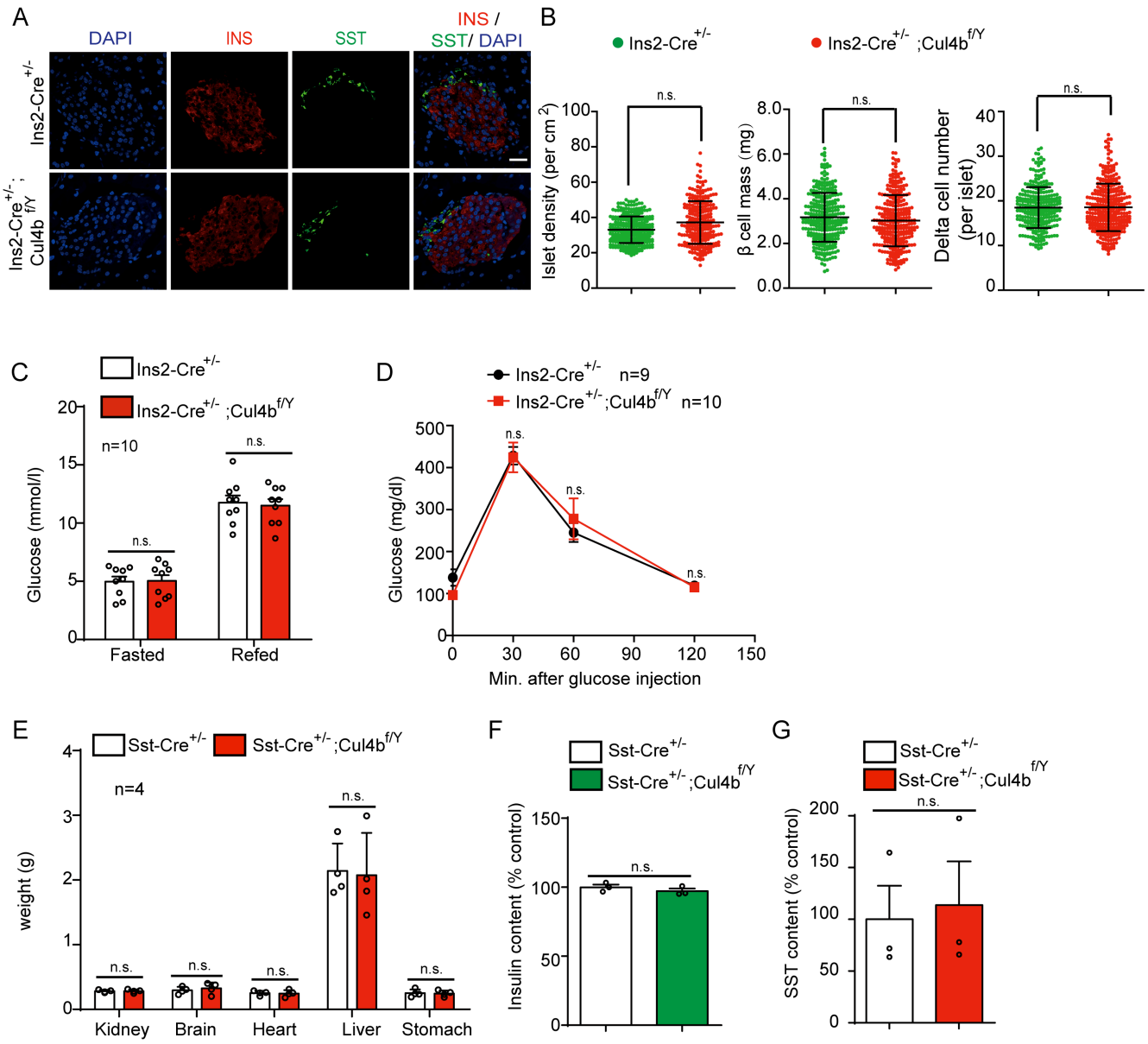

Supplemental Figure 2. (**A**) Immunostaining for SST (green) and insulin (red) in WT and *Ins2-cre; Cul4b*^{flox} mice. Scale bar, 50μm. (**B**) Statistical data indicated there were no significant differences in islet mass, cell number or cell mass between *Ins2-cre; Cul4b*^{flox} mice and their wild type littermates. n=6 mice per group; 4-10 random areas were selected from each pancreatic section, and 12 sections were randomly selected from each mouse. (**C**) There were no significant differences between the fasting and fed blood glucose levels of *Ins2-cre; Cul4b*^{flox} mice and their wild type littermates. n=10. (**D**) Glucose tolerance test for *Ins2-cre; Cul4b*^{flox} mice and their wild type littermates. The *Ins2-cre; Cul4b*^{flox} mice displayed normal glucose tolerance compared with their wild type littermates. n=9-10 (**E**) There were no significant differences in kidney, brain, heart, liver or stomach weights between WT and *SST-cre; Cul4b*^{flox} mice. n=10. (**F-G**) There were no significant differences in insulin or somatostatin content between *SST-cre; Cul4b*^{flox} mice and their wild type littermates. n=5. Error bars in (**B**) represent mean±s.d, other bars represent mean±s.e.m. All data

statistics were analysed using one-way ANOVA.

Supplemental Figure 3

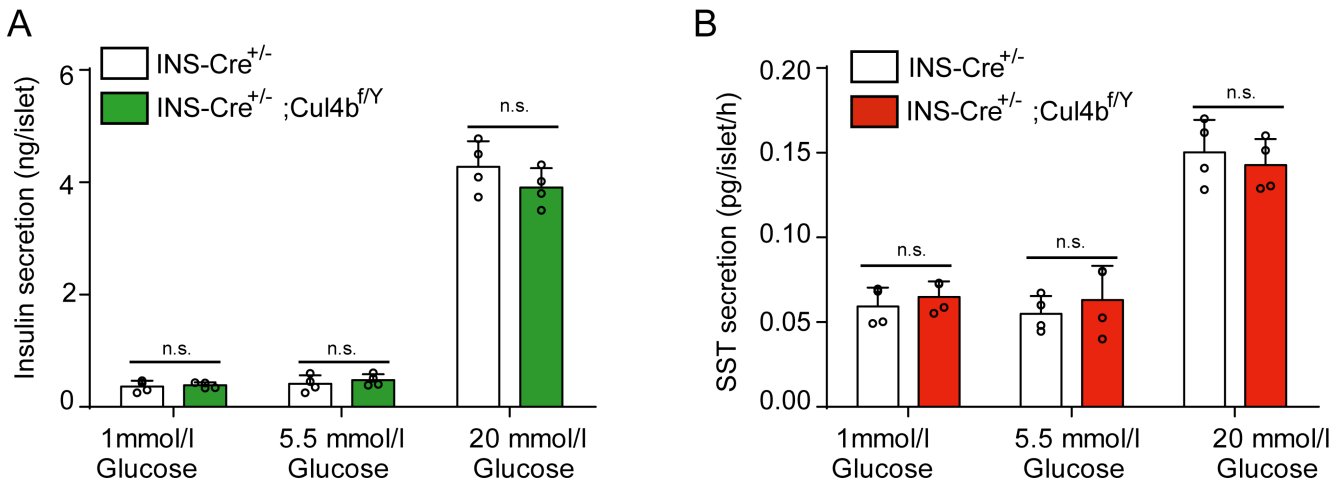

Supplemental Figure 3 (**A-B**) 1 mM, 5.5 mM and 20 mM glucose-induced insulin (**A**) and somatostatin (**B**) secretion in islets isolated from *Ins2-cre; Cul4b*^{flox} mice and their wild type littermates. n=6 mice per group. The bars represent mean±s.e.m. All data statistics were analysed using one-way ANOVA.

Supplemental Figure 4

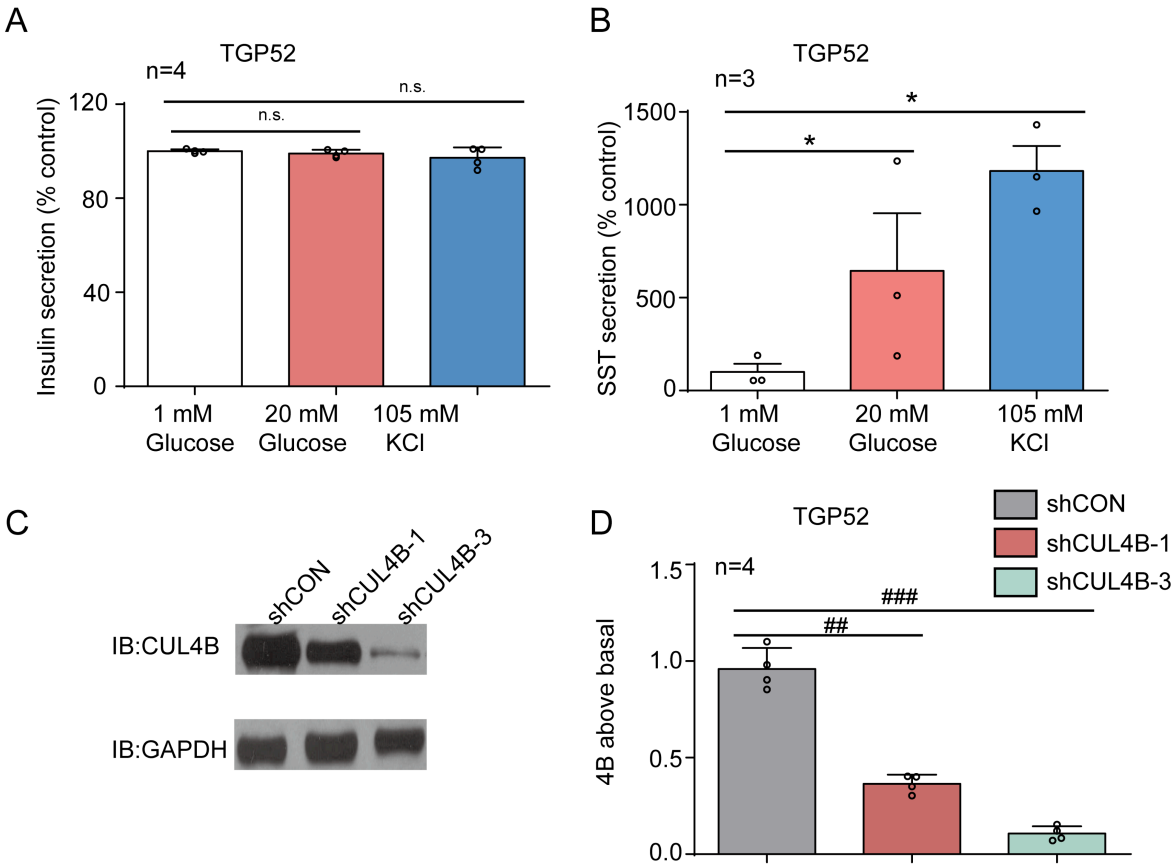

Supplemental Figure 4. (**A**) Glucose- and high KCl-induced insulin secretion from TGP52 cells. Neither high glucose nor high KCl induced significant insulin secretion from TGP52 cells. (**B**) Glucose and high KCl induced significant somatostatin secretion from TGP52 cells. (**C**) The efficiencies of shRNA-mediated CUL4B knockdowns in CUL4B stable cell lines (shCUL4B-1 and shCUL4B-3) were confirmed by western blotting. A representative western blot from at least 3 independent experiments is shown. (**D**) Bar graph and statistical analysis of CUL4B protein levels (analysis of protein levels from **C**). (*p < 0.05; n.s.; no significant differences; the high glucose- or high KCl-stimulated cells were compared with non-stimulated cells. ##, p<0.01; ###p<0.005; the CUL4B protein levels in shCUL4B stable cell lines were compared with those of shCON stable cell lines. The bars represent mean±s.e.m. All data statistics were analysed using one-way ANOVA.

Supplemental Figure 5

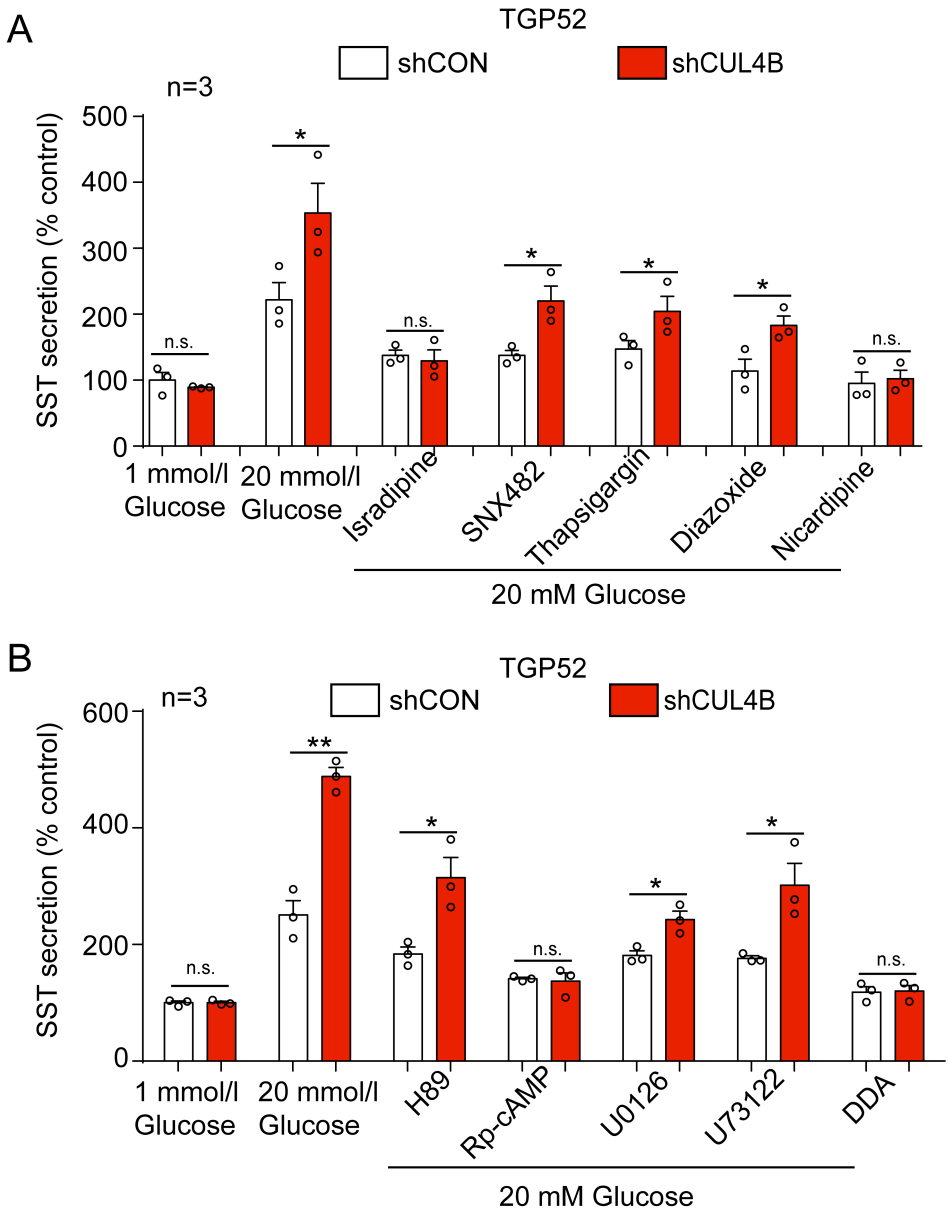

Supplemental Figure 5. (**A**) Glucose-induced somatostatin secretion in CUL4B knockdown and control TGP52 cells in the absence or presence of an R-type calcium channel blocker (100 nM SNX482), L-type channel blockers (10 μM isradipine and 10 μM nicardipine), a potassium/ATP channel opener (250 μM diazoxide) or an inhibitor of an ER ATPase (10 μM thapsgargin). (**B**) Glucose-induced somatostatin secretion in cul4b knockdown and control TGP52 cells in the presence of inhibitors for PKA (10 μM H89), cAMP (100 μM Rp-cAMPs), ERK signaling (10 μM U0126), PLC (10 μM U73122) or adenylyl cyclase (100 μM DDA) inhibitors. *p<0.05; **p<0.01; ***p<0.001; CUL4B knockdown cells were compared with control shRNA knockdown cells. The bars represent mean±s.e.m. All data statistics were analysed using one-way ANOVA.

Supplemental Figure 6

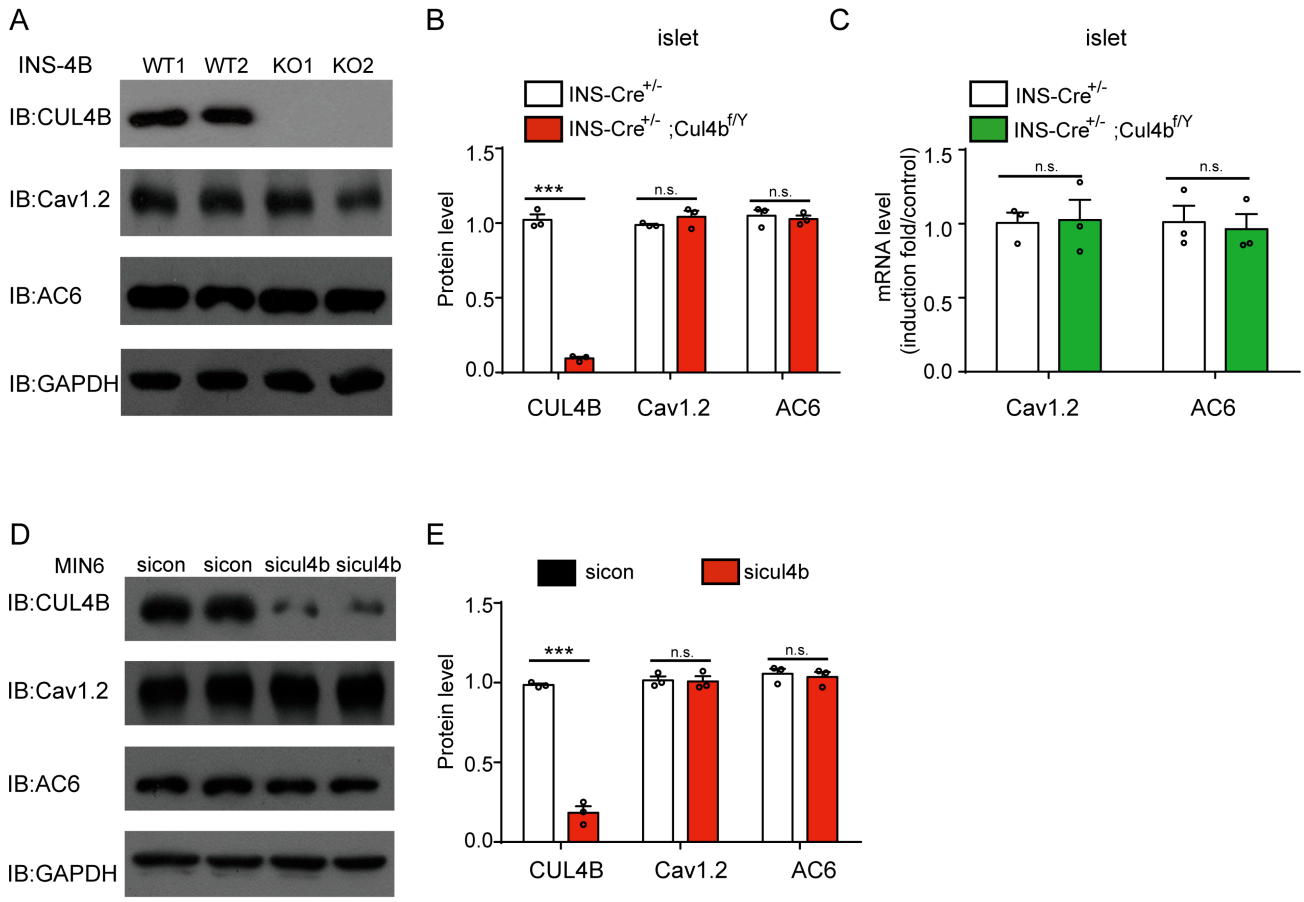

Supplemental Figure 6. (**A**) CUL4B, Cav1.2 and AC6 protein levels in islets isolated from *Ins2-cre; Cul4b^{flox}* mice and their wild type littermates. representative western blots from at least 3 experiments are shown. (**B**) bar graph representation and statistical analyses of (**A**). (**C**) The mRNA levels of Cav1.2 and AC6 in islets isolated from Ins2-cre; Cul4b^{flox} mice and their wild type littermates as determined by q-RT-PCR. (**D**) Cul4b, Cav1.2 and AC6 protein levels in cul4b knockdown and control MIN6 cells. representative western blots from at least 3 experiments

are shown. (**E**) bar graph representation and statistical analyses of (**D**). The bars represent mean±s.e.m. All data statistics were analysed using one-way ANOVA.

Supplemental Figure 7

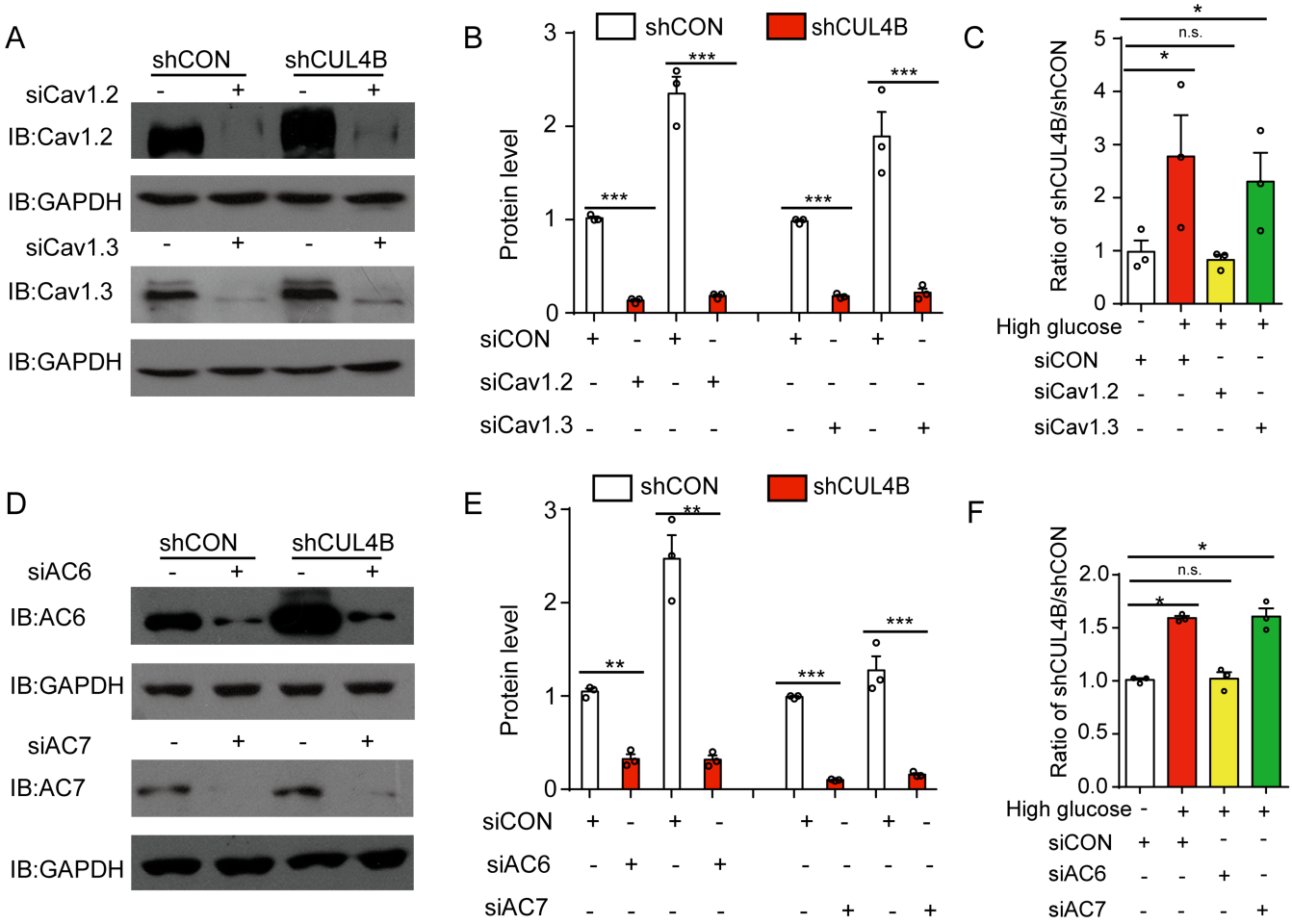

Supplemental Figure 7. (**A-F**) The effect of Cav1.2, Cav1.3, AC6 or AC7 knockdown on the ratio of somatostatin secretion from CUL4B knockdown TGP52 cells versus control cells. A representative western blot from at least 3 independent experiments is shown (**A** and **D**). (**B** and **E**) Bar graph and statistical analysis depicting results from **A** and **D**, respectively. (**C** and **F**) Ratio changes depict the results presented in Figure **4G** and **4H**, respectively. *p<0.05; **p<0.01; ***p<0.001; ns., no significant difference; the Cav1.2, Cav1.3, AC6 or AC7 siRNA-treated cells were compared with control siRNA-treated cells. The bars represent mean±s.e.m. All data statistics were analysed using one-way ANOVA.

Supplemental Figure 8

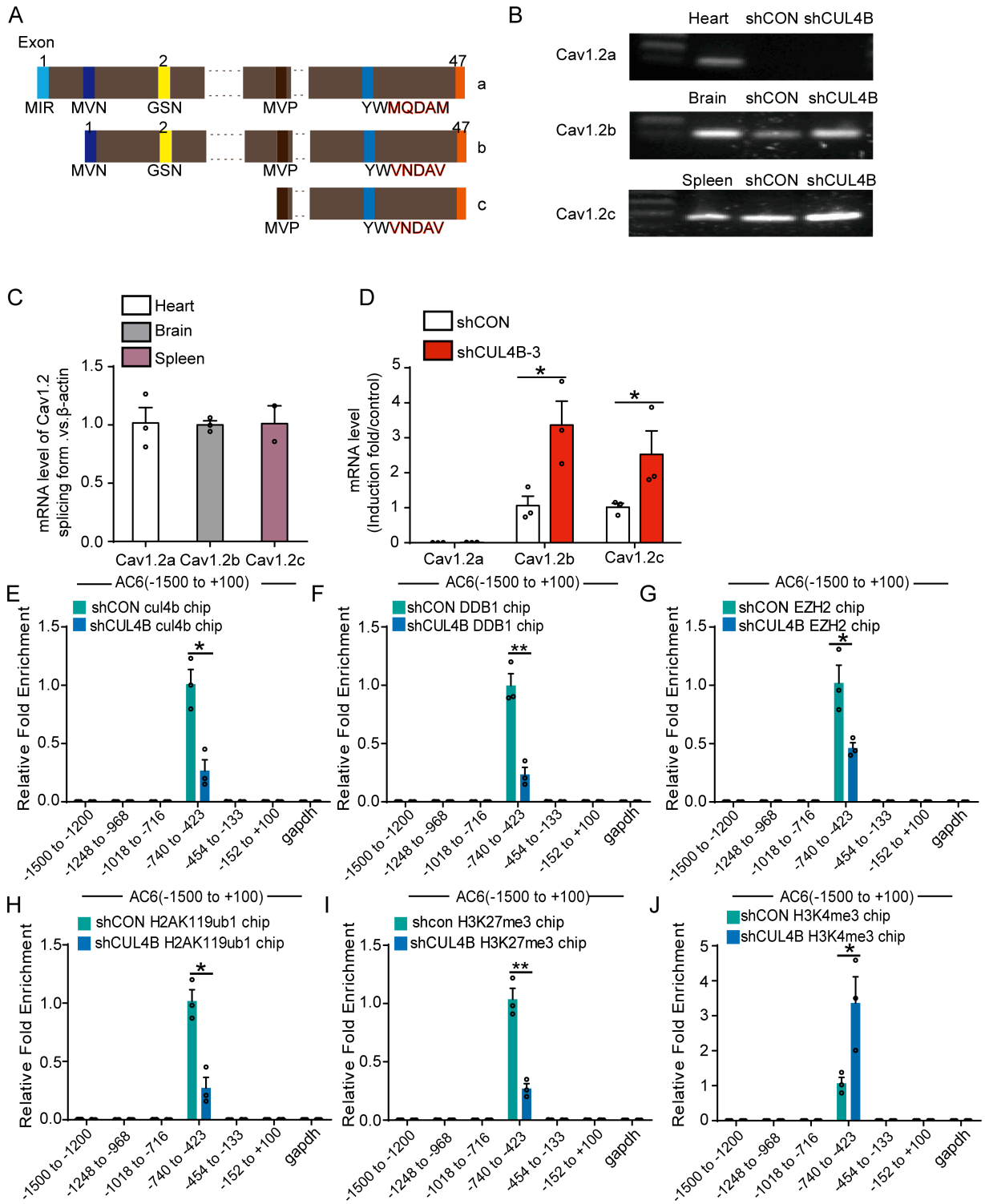

Supplemental Figure 8. (**A**) Schematic representation of the alternatively spliced Cav1.2 mRNA isoforms, including Cav1.2a, Cav1.2b and Cav1.2c. (**B**) The mRNA levels of Cav1.2a, Cav1.2b and Cav1.2c in the heart, brain and spleen of CUL4B knockdown TGP52 cells and control cells by RT-PCR. (**C**) The mRNA levels of Cav1.2a, Cav1.2b and Cav1.2c were analyzed by quantitative RT-PCR and normalized to that of β-actin. (**D**) Quantitative RT-PCR analysis of Cav1.2a, Cav1.2b and Cav1.2c mRNA levels in CUL4B knockdown versus control TGP52 cells. Knockdown of CUL4B significantly increased the mRNA expression levels of Cav1.2b and Cav1.2c. (**E-J**) qChIP analysis of the

recruitment of the indicated proteins to specific regions of the AC6 promoter in CUL4B knockdown and control TGP52 cells. The data indicate the means ± SDs of at least three independent experiments. *, p<0.05; **, p<0.01; ns., no significant difference; the cul4b knockdown cells were compared with control cells. The bars represent mean±s.e.m. All data statistics were analysed using one-way ANOVA.

Supplemental Figure 9

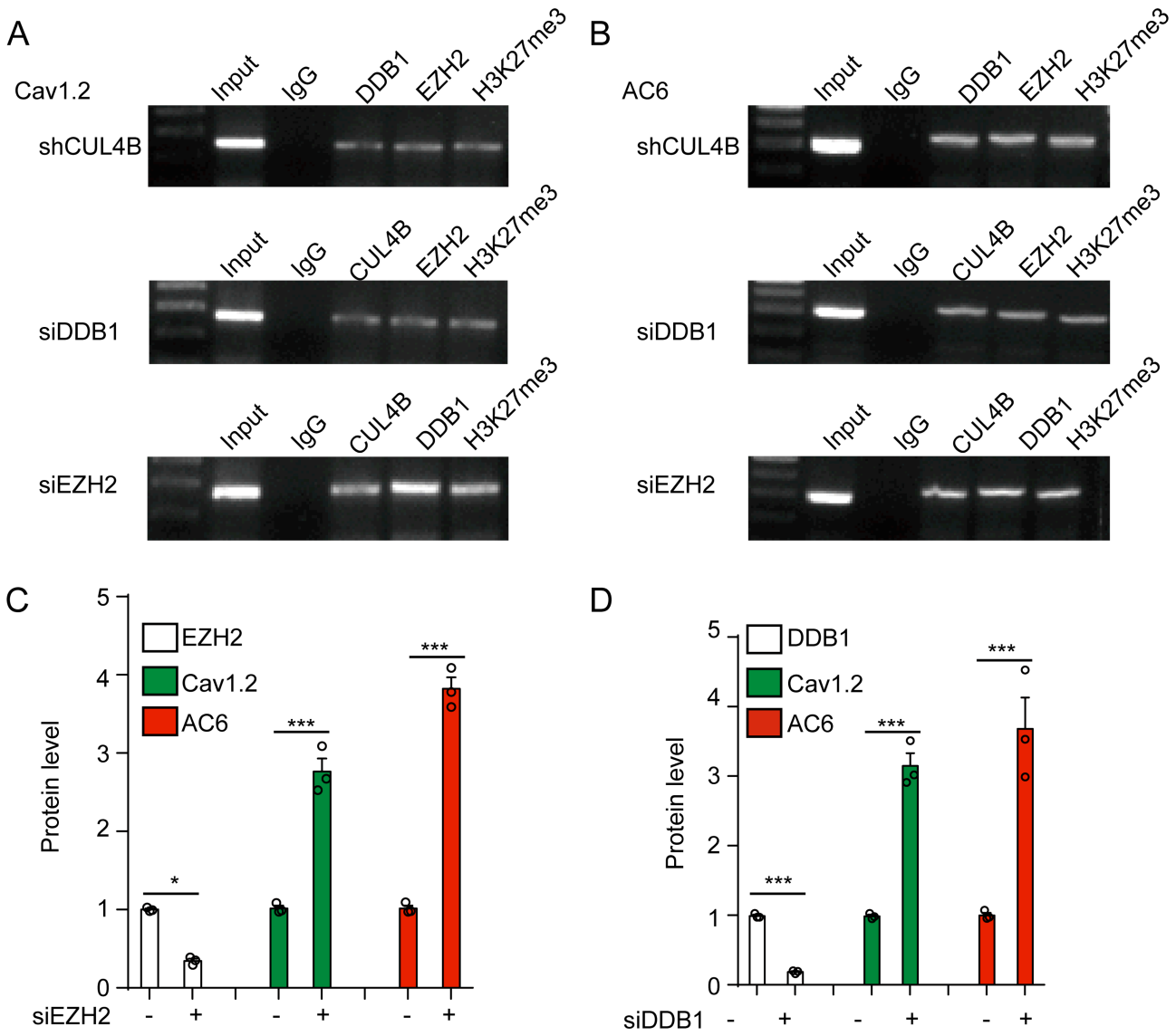

Supplemental Figure 9. (**A, B**) The effect of knockdown of one of the components of the CRL4B/PRC2 complex on the qChIP results of the Cav1.2 (**A**) or AC7 (**B**) promoters immunoprecipitated with the indicated antibodies. A typical reverse transcriptional result is shown. These figures correspond to Figure **6C** and **6D** in the main text. (**C, D**) Bar graph representation and statistical analysis of the western blot from Figure **6E** and **6F**. *, p<0.05; *** p<0.001; n.s. no significant difference; DDB1 and EZH2 knockdown cells were compared with control siRNA-treated cells. The bars represent mean±s.e.m. All data statistics were analysed using one-way ANOVA.

Supplemental Figure 10

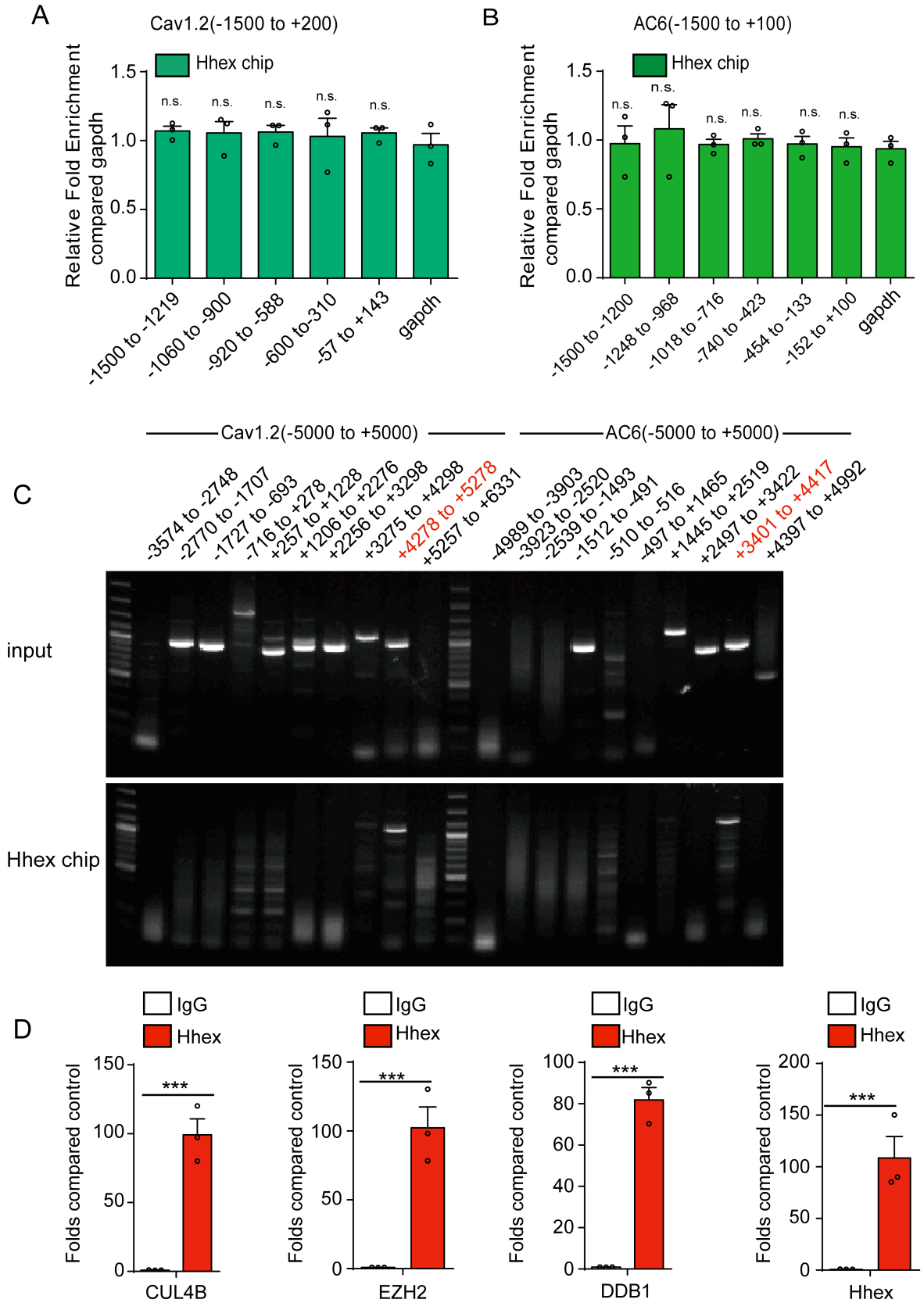

Supplemental Figure 10. (A, C) qChIP analysis of the recruitment of Hhex on specific regions of the cav1.2 and AC6 promoter in TGP52 cells. (**D**) Bar graph representation and statistical analysis of the western blot from Figure

5M. *, p<0.05; *** p<0.001; n.s. no significant difference; Hhex output cells were compared with control cells. The bars represent mean±s.e.m. All data statistics were analysed using one-way ANOVA.

Supplemental Figure 11

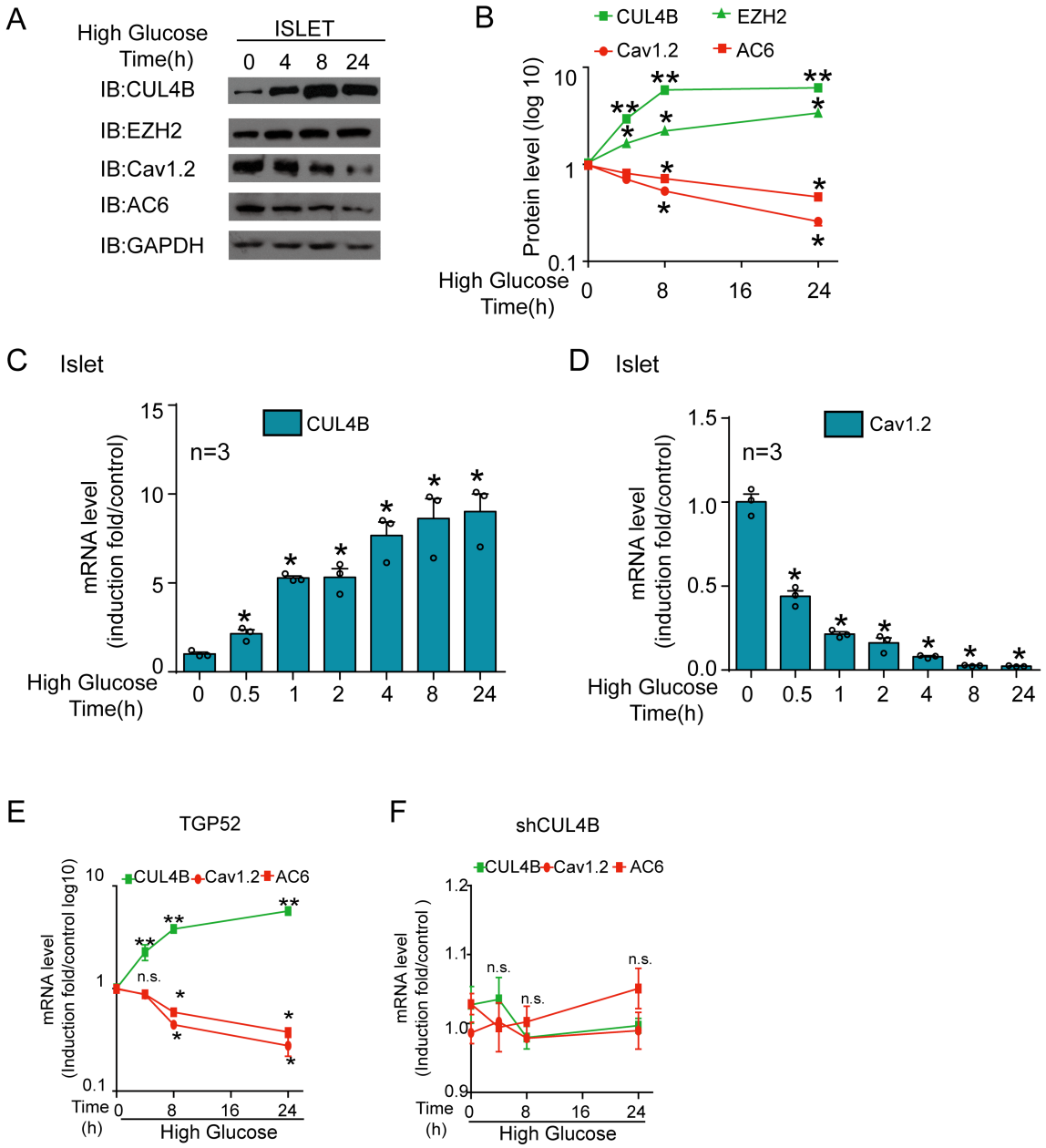

Supplemental Figure 11. (**A-B**) CUL4B, EZH2, Cav1.2 and AC6 expression levels in islets treated with 20 mM glucose for 0, 4, 8 and 24 hours. A representative western blot from at least 3 independent experiments is shown (**A**). Statistical analysis of the data presented in (**B**), which indicated that high glucose promoted CUL4B and EZH2 expression, and decreased Cav1.2 and AC6 expression. (**C**) Quantitative RT-PCR analysis of *Cul4b* mRNA levels in islets treated with 20 mM glucose for 0, 0.5, 1, 2, 4, 8 and 24 hours. (**D**) Whereas continuous high glucose (20 mM) stimulated CUL4B expression in pancreatic islets, Cav1.2 expression exhibited reciprocal reductions. (**E-F**) Q-RT-PCR was used to measure the mRNA levels of Cul4b, Cav1.2 and AC6 in CUL4B knockdown TGP52 cells (**F**)

and control cells (**E**) stimulated with 20 mM glucose for the indicated time intervals. *p<0.05; **p<0.01; ***p<0.001; ns., no significant differences; high glucose- and insulin-treated cells were compared with control cells. The bars represent mean±s.e.m. All data statistics were analysed using one-way ANOVA.

Supplemental Figure 12

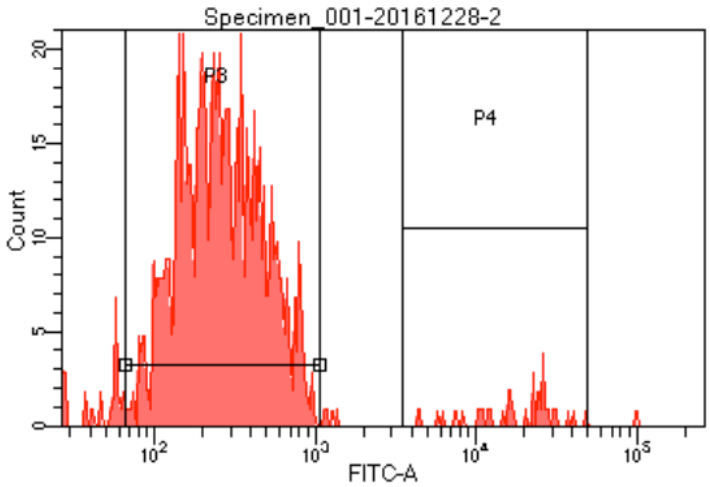

Supplemental Figure 12. The plot of FACS sorting. Approximately 5000 cells from *SST-cre; GFP^{flox}; cul4b^{flox}* mice and their wild type littermates were indicated, then were sorted for GFP expression (P4).

Supplemental Tables

Supplemental Table-1: Primers for ChIP

Gene	Strand	Sequence
Cav1.2-1	F	CAAGCAAGGTGGGCTGTACC
Cav1.2-1	R	CAGGCAGGAAGCCGATTGTAG
Cav1.2-2	F	CTACAATCGGCTTCCTGCCTG
Cav1.2-2	R	GTCCCAGATGGTGATTAAGTGTG
Cav1.2-3	F	GCACGCACCAGGTTTACCATG
Cav1.2-3	R	GTCCCAGATGGTGATTAAGTGTG
Cav1.2-4	F	CCTGGGATGTAGAAGCGAATAC
Cav1.2-4	R	GGTACAGAATCAATCACCTCTC
Cav1.2-5	F	GATTCTGTACCGACTGCTAAAC
Cav1.2-5	R	CCATGTGCTGTGAGCTGTTC
Cav1.2-6	F	GCAATTCTCTGGCACTCTTCC
Cav1.2-6	R	TCATGTAGCCCTGGCTCTG
Cav1.1-1	F	GAACAGTGGTGTTCGAGGTC
Cav1.1-1	R	GAATGCAAGCAGCTGCCTG
Cav1.1-2	F	CAGGCAGCTGCTTGCATTC

Cav1.1-2	R	CATTGCAAGGTGGAGGGTG
Cav1.1-3	F	CTATGCCCACCCTCCACCTTG
Cav1.1-3	R	CTCCACTCACACCAGTCTCAGTG
Cav1.1-4	F	CACTGAGACTGGTGTGAGTGGAG
Cav1.1-4	R	GATTACTCTCTCTGCTCCCAGCG
Cav1.1-5	F	CGCTGGGAGCAGAGAGAGTAATC
Cav1.1-5	R	GCTCCATCTCGCTCAGGTGC
Cav1.3-1	F	GCACACACACAAACTCACACAG
Cav1.3-1	R	CTTGCAGCCTGCCAAGTATC
Cav1.3-2	F	GATACTTGGCAGGCTGCAAG
Cav1.3-2	R	GCTACTCTCTATCTTCCCATCC
Cav1.3-3	F	GGATGGGAAGATAGAGAGTAGC
Cav1.3-3	R	CATAATTAGAGCCGGGTGTGG
Cav1.3-4	F	CCACACCCGGCTCTAATTATG
Cav1.3-4	R	GCTAGCTTTCCAGACATGCAC
Cav1.3-5	F	GTGCATGTCTGGAAAGCTAGC
Cav1.3-5	R	ACATAGATCCCTGGGTTATCATC
Cav1.4-1	F	AGACACGTTCATCTTCCAAGC
Cav1.4-1	R	AGGGAGGATCGACCTCAG
Cav1.4-2	F	GTCCTCTGACATCTACACATG
Cav1.4-2	R	AGCACTACTGGATAGTAGAGAC
Cav1.4-3	F	GTCTCTACTATCCAGTAGTGCT
Cav1.4-3	R	GACAACAAGATGGGAGGGC
Cav1.4-4	F	GCCCTCCCATCTTGTTGTC
Cav1.4-4	R	CACCAAGCAGGCAGAAACC
AC6-1	F	CTCCTTAGCTCACACACACAC
AC6-1	R	GAGGCAGGTGAATTTCTGAGTTC
AC6-2	F	CTCACTTTGTAGACCAGGCTGG
AC6-2	R	GGATCTCTGCCTGACTCGTC
AC6-3	F	GAAGCAATGGCTGTGTGAAGAG
AC6-3	R	CAGATCTCAGGTTCAGACAGG
AC6-4	F	CCTGTCTGAACCTGAGATCTG
AC6-4	R	CAGGTCAACACTTGTGGTAAGG
AC6-5	F	CCTTACCACAAGTGTTGACCTG
AC6-5	R	CAAGCAGCTGCCCAAGTTAC
AC6-6	F	GTAACTTGGGCAGCTGCTTGCG
AC6-6	R	GCAAACCTGCTGCGCACAGAAC
AC7-1	F	GGACAACATTTAACTGGGGCTGGC
AC7-1	R	GACATGGCCAAGGTGACACTTGC
AC7-2	F	GCAAGTGTCACCTTGGCCATGTC
AC7-2	R	GTGGGATCTGCGTGATCCTGG
AC7-3	F	GTTCCAGGATCACGCAGATC
AC7-3	R	CACAACTCTACTGACCTGAAGG
AC7-4	F	CCTTCAGGTCAGTAGAGTTGTG
AC7-4	R	GCCTTAGGTCACCAGCCAG
AC7-5	F	GACCACGTGGGAGAGGTAC
AC7-5	F	GCTGGTCACACTGACCGTG

Supplemental Table-2: Primers for qPCR

Cul4A	F	TCTCACAAAGTCTCCCCAACG
Cul4A	R	AGGACGTAGGTTCGATCCAGA
Cul4B	F	TGCTGGCAAAACCACTGTAGG
Cul4B	R	CCAAATGGAGGGTAGCATTGAA
Cul1	F	CTCAGTTTGTTGGCTTGGAGT
Cul1	R	TGGAGAATCGGTAATCTTCCCA
Cul3	F	CAGTCCCTCGCCTGTGGTA
Cul3	R	TGGCTGCAACTGTTTGAATCT
Cav1.1	F	TCAGCATCGTGGAATGGAAAC
Cav1.1	R	GTTCAGAGTGTTGTTGTCATCCT
Cav1.2	F	TTGAGCAACCTTGTGGCATCCTTG
Cav1.2	R	ACGGGTCTGCATCTCATCGAAGTT
Cav1.3	F	GCAAACTATGCAAGAGGCACC
Cav1.3	R	GGGAGAGAGATCCTACAGGTGG
Cav1.4	F	GTGGAGAGAATGAGGACGCAA
Cav1.4	R	TCCGAAGCGGGTTGGTTTG
AC1	F	TGCTCTTCTTTGGTGTGAAC
AC1	R	CTCAATGCAGTTTCGAGCC
AC2	F	GACTGGCTCTACGAGTCCTAC
AC2	R	GGGCAGTGGGAACGGTTAT
AC3	F	CTCGCTTTATGCGGCTGAC
AC3	R	ACATCACTACCACGTAGCAGT
AC4	F	AGTACCCACTGCTGATACTGC
AC4	R	AGCCACCCAAAGCACACAG
AC5	F	CTTGGGGAGAAGCCGATTCC
AC5	R	ACCGCTTAGTGGAGGGTCT
AC6	F	GTACTCATGGTGGTGTGTAACC
AC6	R	GGTGATGTAGACGAAGAACACG
AC7	F	AAGGGGCGCTACTTCCTAAAT
AC7	R	GTGTCTGCGGAGATCCTCA
AC8	F	CACTTACCTGCAATACAGCG
AC8	R	AGGTGGCGAAGAGTGTAAAA
Gs	F	GCAGCGCGAGGCCAACAAAAA
Gs	R	GGTCCTCTTCGCCGCCCTCTC
PKA	F	AGCAGGAGAGCGTGAAAGAG
PKA	R	CCAGCTTAACCACTGCAAAA
pdk1	F	GGACTTCGGGTCAGTGAATGC
pdk1	R	TCCTGAGAAGATTGTCGGGGA
mafa	F	AGGAGGAGGTCATCCGACTG
mafa	R	CTTCTCGCTCTCCAGAATGTG
hhex	F	CGGACGGTGAACGACTACAC
hhex	R	CGTTGGAGAACCTCACTTGAC
pax6	F	TACCAGTGTCTACCAGCCAAT
pax6	R	TGCACGAGTATGAGGAGGTCT
ngn3	F	CCAAGAGCGAGTTGGCACT

ngn3	R	CGGGCCATAGAAGCTGTGG
pdx1	F	CCTTTCCCGAATGGAACCGA
pdx1	R	GGGCCGGGAGATGTATTTGT
mafb	F	TGGATGGCGAGCAACTACC
mafb	R	CCAGGTCATCGTGAGTCACA
nkx6.1	F	CTGCACAGTATGGCCGAGATG
nkx6.1	R	CCGGGTTATGTGAGCCCAA

Supplemental Material and Methods

Antibodies and Reagents.

The anti-CUL4B antibody (c9995) was purchased from Sigma. The anti-CUL4A antibody (14851-1-AP), anti-ADCY6 antibody (14616-1-AP) and anti-Cav1.1 antibody were bought from Proteintech. The anti-Cav1.2 antibody (ACC-003) and anti-Cav1.3 antibody (ACC-005) were purchased from Alomone. The anti- ADCY7 (sc-25501) antibody and anti-Ddb1 (sc-25367) antibody were purchased from Santa Cruz Co. The anti-EZH2 (612666) antibody was purchased from BD Transduction Laboratories, the anti-trimethyl H3-K4, and anti-trimethyl H3-K27 antibody were purchased from Millipore, and the anti-Hhex (ab34222) antibody was obtained from Abcam. For immunofluorescence, the anti-insulin antibody (sc-9168) and anti-somatostatin antibody (sc-7819) were purchased from Santa Cruz Co. The secondary antibodies we utilized were Alexa Fluor 488 and Alexa 594 (Invitrogen, Camarillo, CA). The DAPI (C1002) was provided by Beyotime. The Cyclosomatostatin, SNX482, Isradipine, Nicardipine and MG132 were purchased from Abcam. The Rp-cAMP, Tharpsigargin, Diazoxide, DDA, Ast2B and Ucn3 were bought from Sigma-Aldrich. Collagensae P and SYBR Green were purchased from Roche. All other chemical or reagents were supplied by Sigma unless otherwise specified.

Islet isolation, dispersion, and culture

Pancreatic islets cells were isolated from differential genotypic adult mice and cultured as described previously(1). Briefly, adult mice were killed by cervical dislocation and pancreata were isolated from them individually. Adult pancreata were digested by collagensae P at 37 °C for 17-18 minutes. Digestion was teminated by Hank's balanced salt solution (136.9 mmol/l NaCl; 5.4 mmol/l KCl; 1.3 mmol/l $CaCl_2$; 0.8 mmol/l $MgSO_4$; 0.44 mmol/l KH_2PO_4; 0.34 mmol/l Na_2HPO_4; 5.55 mmol/l D-glucose; 4.4 mmol/l $NaHCO_3$, pH=7.35-7.45) followed by sedimentation which was at 4°C for 4 minutes each time. Finally, islets were collected by hand picking by a stereomicroscope. For all primary islet cell experiments, islets were cultured overnight in islet complete media containing 1000 mg/l glucose, 10% v/v FBS, 0.1% v/v penicillin/streptomycin. Then islets were hand-picked to three or six groups and each group has thirty islets. Each group was cultured in modified KRBB buffer (120 mmol/l NaCl, 5 mmol/l KCl, 2 mmol/l $CaCl_2$, 1 mmol/l $MgCl_2$, 24 mmol/l $NaHCO_3$ and 15 mmol/l HEPES at pH 7.42) for 1 hour starvation. After that, every group were stimulated with glucose, insulin or high KCl in mKRBB buffer for western blot, quantitative PCR and ELISA experiments.

Cell isolation and FACS purification

The *SST-cre; GFP^{flox}*; *cul4b^{flox}* mice and their wild type littermates were sacrifice firstly, then islets were isolated with collagensae P (Roche), and then the single pancreatic cells were obtained with 0.6U/ml Dispase II enzyme followed by filtration on a 40 μm nylon mesh. Approximately 5000 cells from *SST-cre; GFP^{flox}; cul4b^{flox}* mice and their wild type littermates were indicated, then were sorted for GFP expression. Six age-matched (12-14 weeks old) mice were used per genotype per sorting. Cell sorting was performed by the FACS service at Shandong University School of Medicine.

Somatostatin measurement

Thirty islets were treated with high glucose, other agonists or antagonists, for the indicated time points and the supernatant fraction was also collected to measure the secreted fractions. The islets were boiled at 100°C for 15 min to measure the cellular somatostatin content. The somatostatin levels were measured with the Phoenix Pharmaceuticals ELISA kit (EK-060-03), as what indicated by the manufacturer's instructions.

Insulin measurement

Thirty islets were treated with high glucose, other agonists or antagonists, for the indicated time points, and the supernatant fraction was also collected to measure the secreted fractions. The islets were lysed with 0.18 N HCl in 70% ethanol to measure the cellular insulin contents. The insulin levels were measured with the Millipore Rat / Mouse Insulin (Cat. # EZRMI-13K), as what indicated by the manufacturer's instructions. Analysis of the results was done using Matlab software.

Cell culture conditions and treatments

TGP52 cells purchased from the American Type Culture Collection (ATCC) (Maryland, USA) and TGP52 knocked down cul4b cells were cultured at 37°C, 5% CO_2 condition and in DMEM: F12 media (ATCC, 17.5 mmol/l glucose, 13 mmol/l HEPES, 2.5 mmol/l L-glutamine, 10% FBS, 100 U/ml penicillin and 100 μg/ml streptomycin) supplemented with 10% FBS, 100 U/ml penicillin and 100 μg/ml streptomycin. Insulin-secreting MIN6 cells were cultured in a DMEM media (25 mmol/l glucose, 2.5 mmol/l L-glutamine, 15% FBS, 50 μmol/l β-mercaptoethanol, 100U/ml penicillin and 100μg/ml streptomycin). NIH3T3 cells were cultured in 25 mmol/l glucose, 10% v/v FBS, 100U/ml penicillin and 100μg/ml streptomycin DMEM media. BV2 cells were cultured in 25 mmol/l glucose, 10% v/v FBS, 100U/ml penicillin and 100μg/ml streptomycin DMEM media without sodium pyruvate. For insulin or high glucose stimulation, the cells were starved for 12 h in low glucose media.

Insulin tolerance test

12-14 Weeks male mice were fasted for 6 h with water available ad libitum, and blood glucose was measured from tail blood before (baseline, 0 min) as well as 30, 60, 90 and 120 minutes after that mice were

intraperitoneally challenged with 0.75 U/kg body weight Novolin Regular Human Insulin (Novo Nordisk Pharmaceuticals Inc., Princeton, NJ).

Immunofluorescence

Briefly, mouse pancreases were dissected and fixed in 4% formaldehyde at 4°C for at least 8 h, then putted in 10% sucrose for 4h, 20% sucrose for 8h, 30% sucrose for 12h, sequentially. The mouse pancreases slices were incubated at 4°C with blocking buffer for 90-120 minutes, then incubated overnight at 4°C with anti-insulin (santa, 1:250), anti-somatostatin (santa, 1:500), and anti-CUL4B (SIGMA, 1:1000). After washing three times with PBS, the slices were incubated at 4°C with secondary antibodies Alexa Fluor 488 and Alexa Fluor 555 (Invitrogen). Finally the slices were stained with 4′,6-diamidino-2-phenylindole and left in the dark before fluorescence microscopic analysis.

Detection of ubiquitinated Cav1.2 and AC6

TGP52 cells and TGP52 knocked down cul4b cells were cultured in 10 cm cell culture dishes and transfected with HA-ubiquitin(2). Two days after transfection, the cells were treated with proteasome inhibitor (MG132, 10 nM) for 6 h. The cells were then scraped and resuspended in lysis buffer. After 2 h of end-over-end rotation at 4°C, the lysate was cleared by high-speed centrifugation. The soluble lysate were incubated with 20 μl HA affinity beads for overnight. The beads were washed at least three times with lysis buffer and then resuspended with lysis buffer. The ubiquitinated Cav1.2 and AC6 were detected by specific antibodies.

Western blotting

TGP52 Cells were washed with cold PBS and lysed in cold lysis buffer (20 mM HEPES, 420 mM NaCl, 1.5 mM $MgCl_2$, 0.2 mM EDTA, 10 mM Na_3VO_4, 10 mM NaF, 25% (v/v) glycerol, protease inhibitor cocktail) for 20 minutes at 4°C. After centrifugation at 13800×g at 4°C for 30 min, the protein concentration was quantified by the Bradford protein assay. Equal amounts of lysate proteins were denatured in 2×loading buffer and boiled at 100°C for 10min. Proteins were probed by loading 20 μg aliquots (10% gels) under denaturing conditions on SDS/PAGE, followed by wet transfer onto PVDF membranes (Millipore). After transferring to nitrocellulose membranes and blocking, the membranes were incubated with the primary antibody at 4°C with gentle shaking overnight. After washing, the membranes were incubated with the secondary antibody for 2 h at room temperature followed by chemiluminescence detection with the substrate from Pierce. The films were scanned, and the band intensities were quantified using ImageJ software (National Institutes of Health, Bethesda MD).

To detection the expression Cav1.1, Cav1.2, Cav1.3, Cav1.4, TGP52 cells and TGP52 knocked down cul4b cells were cultured in 10 cm cell culture dishes. For preparation of membrane, the TGP52 cells were scraped

cells in 75 mM Tris-HCl pH 7.4, 2 mM EDTA, dounce the cells homogeneous 100-200 times, then centrifuge 1000 rpm 15min to get rid of the unbroken cells and nucleus, get supernatant. After that, centrifuge 17000 rpm 1 hour to get crude membranes, then resuspend the membrane in 75 mM Tris-HCl pH 7.4, 2 mM EDTA, 12.5 mM $MgCl_2$, pipet enough to make homogeneous membrane.

RNAi

For knock down Cav1.2, Cav1.3, AC6, AC7, EZH2 or DDB1, the TGP52 cells were transfected using Opti-MEM medium and Lipofectamine (Invitrogen) according to the manufacturer's instructions. Besides the siRNAs were purchased from Sigma.

Calcium measurement

$[Ca^{2+}]_i$ was measured using a Ca^{2+} imaging system (TILL, Germany). The primary cells were preloaded with fura-2 by incubation in 2 μM fura-2 AM for 30 min at 37°C. The loaded cells were excited at 340 nm and 380 nm alternately(3). The software calculated the F340/F380 ratio, which represents the corresponding $[Ca^{2+}]_i$ change.

cAMP measurement

TGP52 cells and knocked down cul4b cells were cultured in mKRBB buffer for 1hour starvation. After that, every group were sequentially stimulated with 1 mM or 20 mM glucose in mKRBB buffer for 15 minutes. Then the cAMP level was measured according to the manufacturer's protocols (KGE012B, Parameter).

ChIP and ChIP-Re-ChIP

Briefly, 1 x 10^7 cells were cross-linked with 1% formaldehyde. Afterwards, these cells are sonicated, pre-cleared, and incubated with 5-10 μg of antibody per reaction at 4°C overnight. Then the beads were added to bind with the antibody for 2 h at 4°C(4). Complexes were washed with low and high salt buffers, and the DNA was extracted and precipitated. For Re-ChIP assays, the eluates were then diluted 30-fold with ChIP dilution buffer and subjected to a second immunoprecipitation reaction. The final elution step was performed using elution buffer (pH 8.0). The enrichment of the DNA template was analyzed by conventional PCR using primers specific for each target gene promoter

Reference

1. Ning SL, Zheng WS, Su J, Liang N, Li H, Zhang DL, Liu CH, Dong JH, Zhang ZK, Cui M, et al. Different downstream signalling of CCK1 receptors regulates distinct functions of CCK in pancreatic beta cells. *Br J Pharmacol.* 2015;172(21):5050-67.
2. Wang HM, Xu YF, Ning SL, Yang DX, Li Y, Du YJ, Yang F, Zhang Y, Liang N, Yao W, et al. The catalytic region and PEST domain of PTPN18 distinctly regulate the HER2 phosphorylation and ubiquitination barcodes. *Cell Res.* 2014;24(9):1067-90.

3. Dou HQ, Xu YF, Sun JP, Shang S, Guo S, Zheng LH, Chen CC, Bruce IC, Yu X, and Zhou Z. Thiopental-induced insulin secretion via activation of IP3-sensitive calcium stores in rat pancreatic beta-cells. *Am J Physiol Cell Physiol.* 2012;302(5):C796-803.
4. Ji Q, Hu H, Yang F, Yuan J, Yang Y, Jiang L, Qian Y, Jiang B, Zou Y, Wang Y, et al. CRL4B interacts with and coordinates the SIN3A-HDAC complex to repress CDKN1A and drive cell cycle progression. *J Cell Sci.* 2014;127(Pt 21):4679-91.

Full unedited gel for main figure 1-7

Fig.1

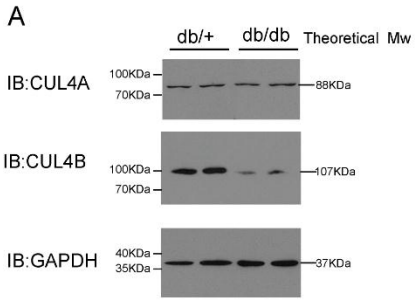

Fig.5

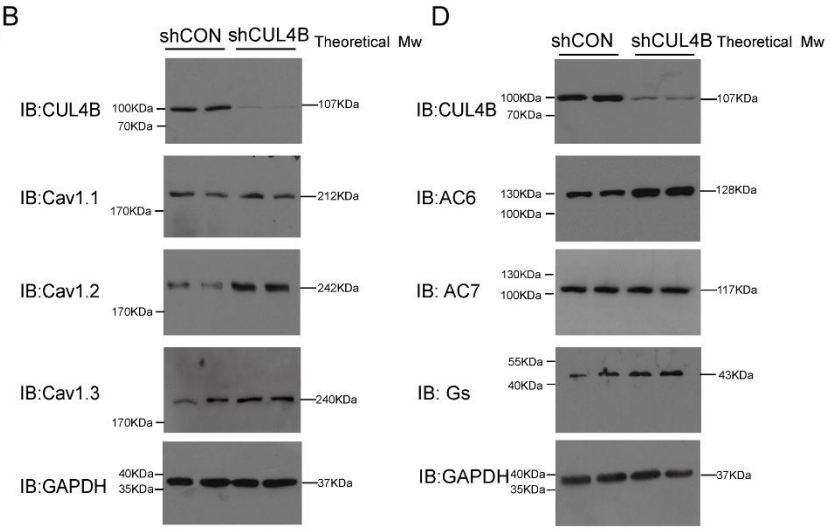

Fig.6

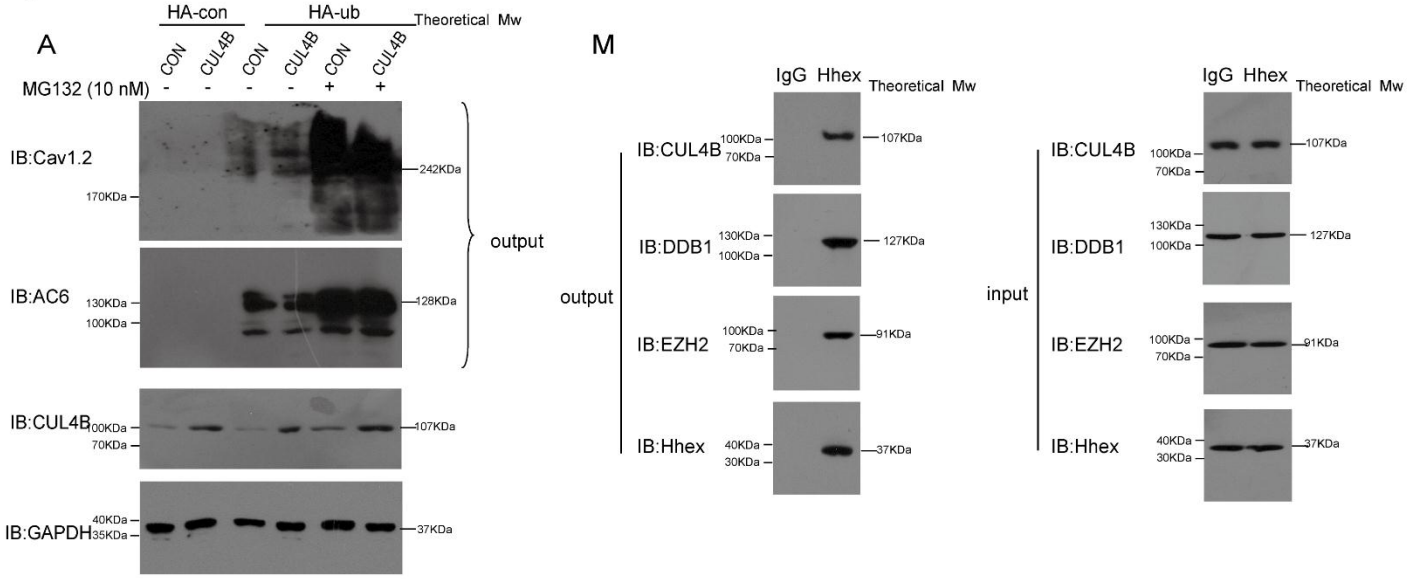

Fig.7

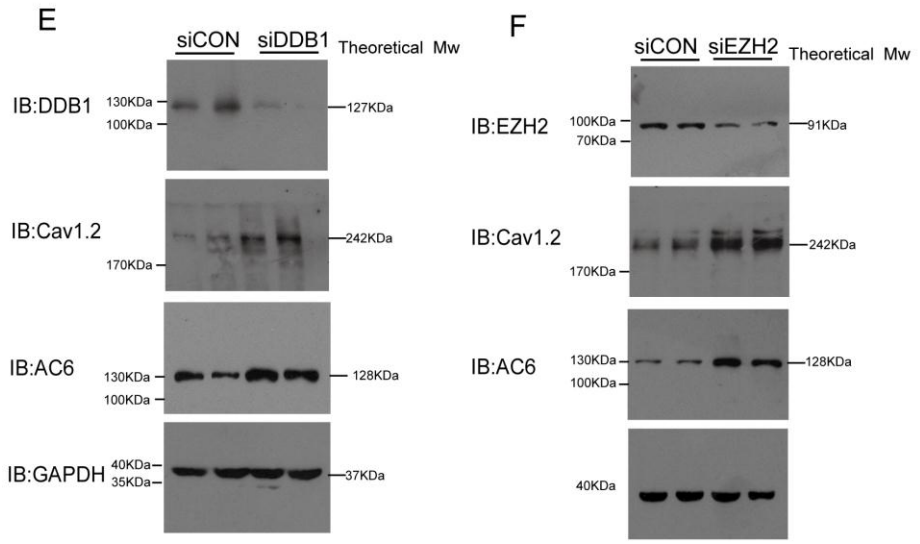
E
siCON
siDDB1
Theoretical Mw
IB:DDB1
130KDa
100KDa
127KDa
IB:Cav1.2
170KDa
242KDa
IB:AC6
130KDa
100KDa
128KDa
IB:GAPDH
40KDa
35KDa
37KDa
F
siCON
siEZH2
Theoretical Mw
IB:EZH2
100KDa
70KDa
91KDa
IB:Cav1.2
170KDa
242KDa
IB:AC6
130KDa
100KDa
128KDa
40KDa

Fig.8

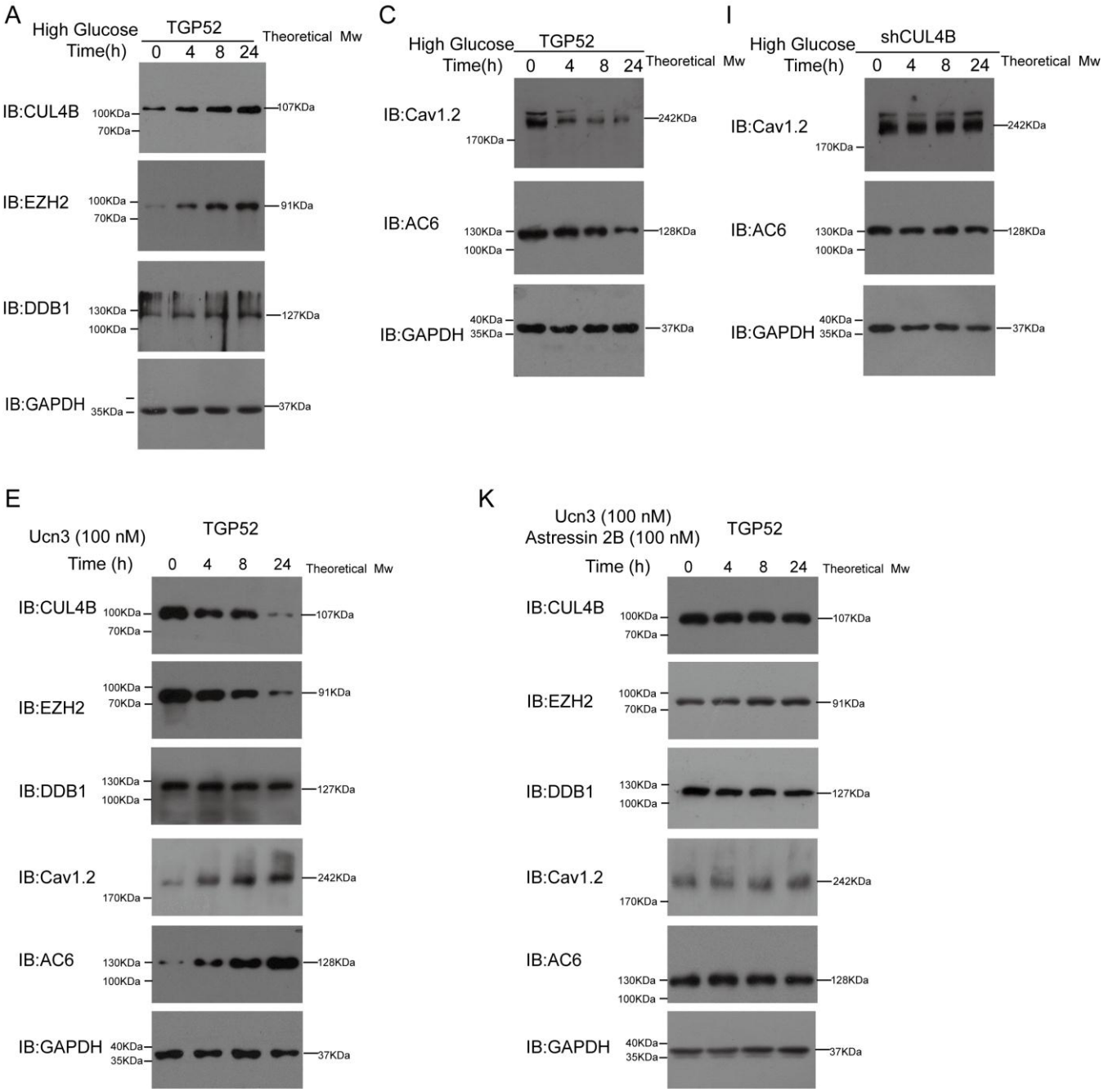
A
High Glucose
Time(h)
TGP52
0 4 8 24
Theoretical Mw
IB:CUL4B
100KDa
70KDa
107KDa
IB:EZH2
91KDa
IB:DDB1
130KDa
100KDa
127KDa
IB:GAPDH
35KDa
37KDa
C
High Glucose
Time(h)
TGP52
0 4 8 24
Theoretical Mw
IB:Cav1.2
170KDa
242KDa
IB:AC6
130KDa
100KDa
128KDa
IB:GAPDH
40KDa
35KDa
37KDa
I
High Glucose
Time(h)
shCUL4B
0 4 8 24
Theoretical Mw
IB:Cav1.2
242KDa
IB:AC6
128KDa
IB:GAPDH
37KDa
E
Ucn3 (100 nM)
Time (h)
TGP52
0 4 8 24
Theoretical Mw
IB:CUL4B
100KDa
70KDa
107KDa
IB:EZH2
91KDa
IB:DDB1
130KDa
100KDa
127KDa
IB:Cav1.2
170KDa
242KDa
IB:AC6
128KDa
IB:GAPDH
40KDa
35KDa
37KDa
K
Ucn3 (100 nM)
Astressin 2B (100 nM)
Time (h)
TGP52
0 4 8 24
Theoretical Mw
IB:CUL4B
100KDa
70KDa
107KDa
IB:EZH2
91KDa
IB:DDB1
130KDa
100KDa
127KDa
IB:Cav1.2
170KDa
242KDa
IB:AC6
128KDa
IB:GAPDH
40KDa
35KDa
37KDa

Full unedited gel for supplemental figures

SFig 1

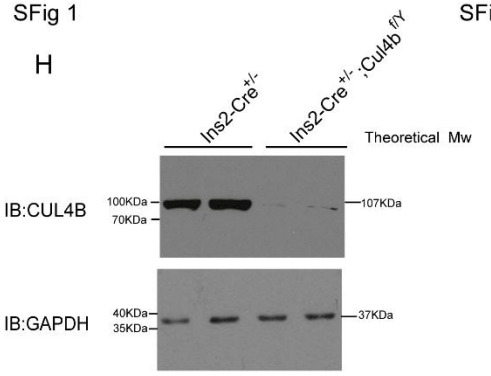

SFig 4

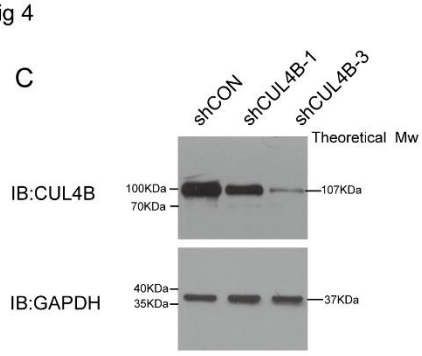

SFig 11

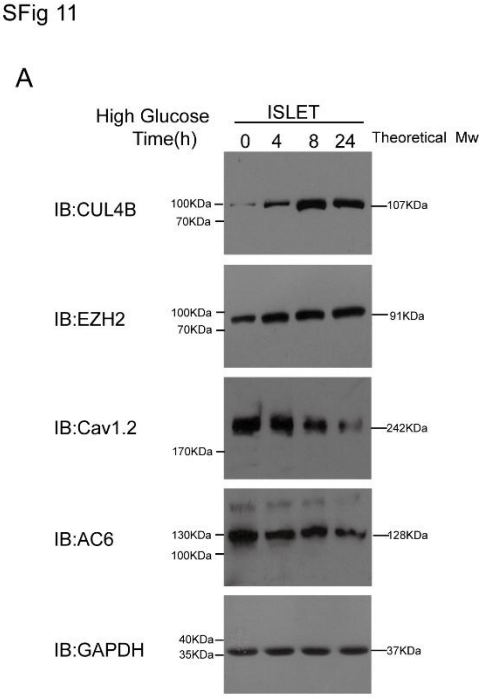

SFig 6

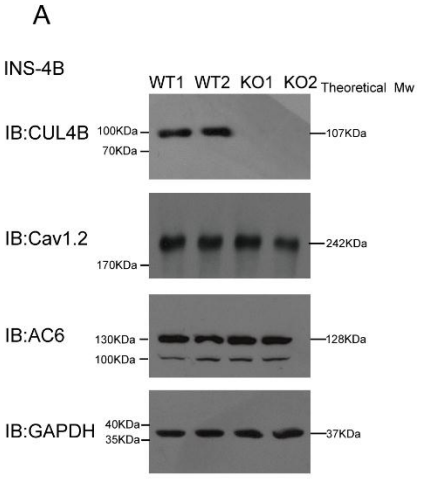

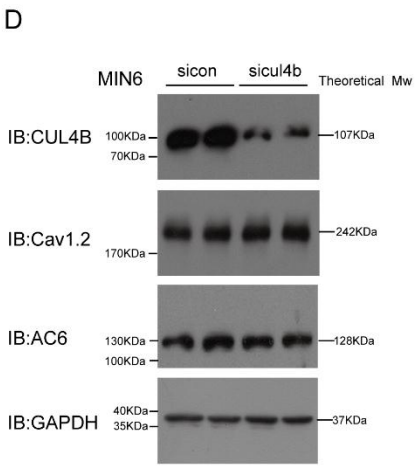

SFig 7

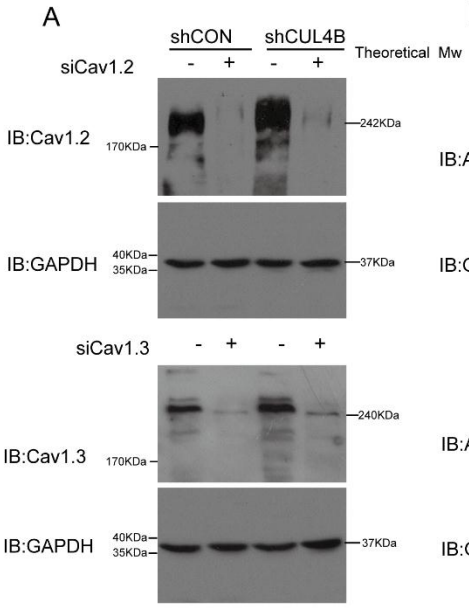

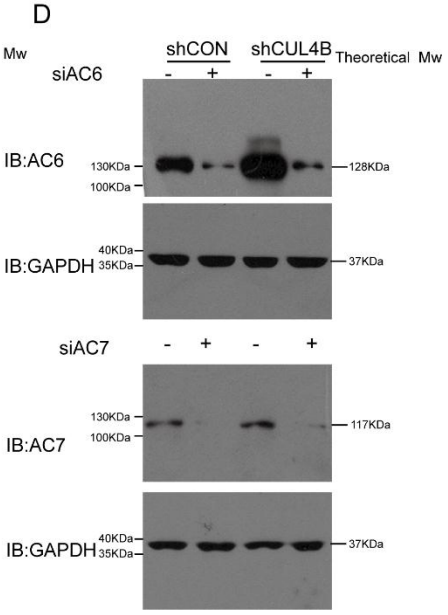

Full unedited gel images

Fig.7

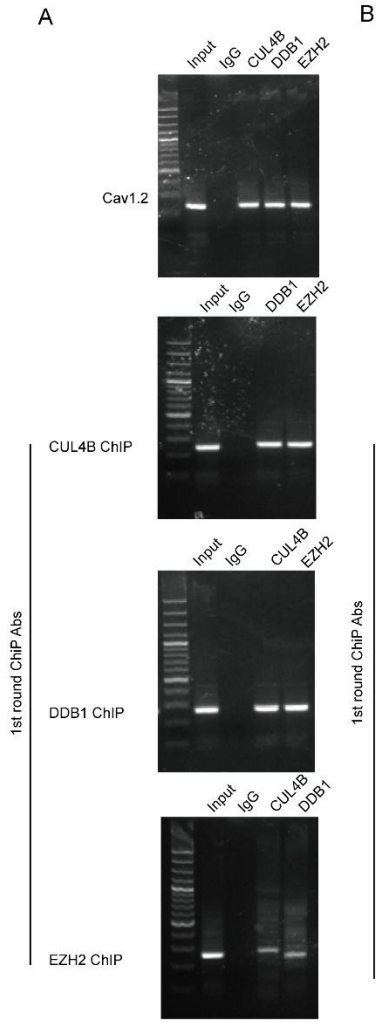

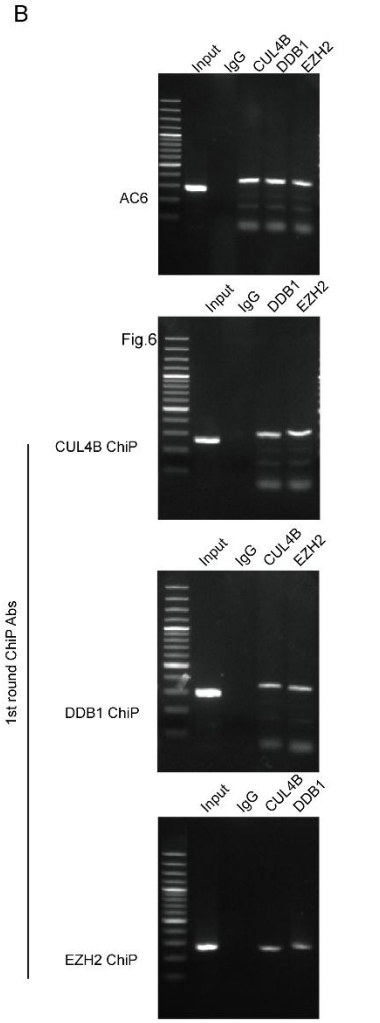

Fig.6

sFig.1

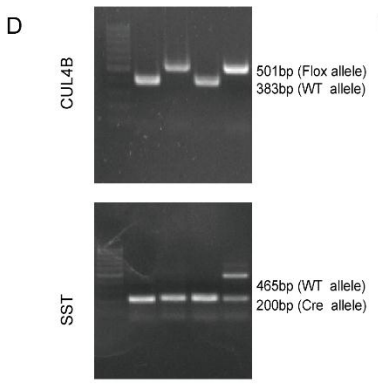

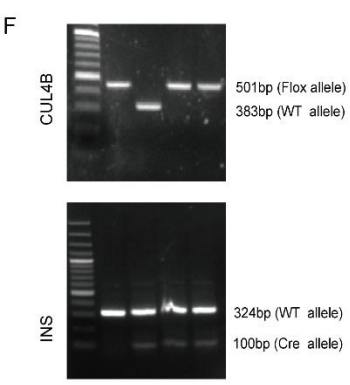

sFig.9

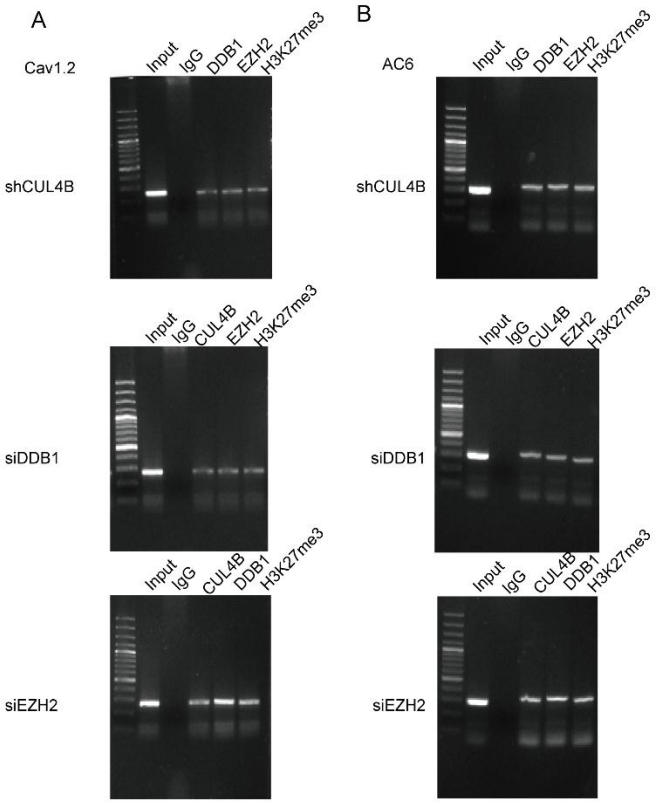

sFig.8